Transactions of the 15th International Conference on
Structural Mechanics in Reactor Technology (SMiRT-15)
Seoul, Korea, August 15-20, 1999

A Method to Build on Improved Stress Field in the Local Region Using the Concept of Conjugate Approximations and Iterative Method

Kee-Nam Song and Heung Seok Kang

Korea Atomic Energy Research Institute, Korea

ABSTRACT: An approximate method to build an improved and continuous stress field in local regions has been proposed, based on the theory of conjugated approximations for the buildup of a continuous stress field and the Loubignac's iterative method for the restoration of momentum balance in a smoothed stress field. The validity of the proposed method has been tested through two examples. Analysis of the examples shows that the stress field obtained for the local region model by the proposed method agrees well with that for the whole domain model. In addition, a significant reduction in the computing time to obtain the improved stress field implies that the proposed method can be an efficient alternative for detailed stress analysis in local regions.

1. INTRODUCTION

After more than four decades of study and development, the displacement-based finite element method that maintains only C^0 continuity over the problem domain has come to be an effective and widely used tool for numerical analysis in the engineering field. In many applications, the quantities of primary interest are not the primary variables, such as displacement and temperature, but rather functions of the derivatives of the primary variables, such as stress, strain, and flux. Since these derivatives do not possess inter-element continuity in the displacement-based finite element method, a number of post-processing techniques have been developed over the years to interpret these discontinuous fields, such as mixed formulations [1], and the projection method [2,3], and an iterative method [4].

So, the objective of the above methods is to get an improved stress field over the entire structure. In particular cases, it is necessary to model a small portion of the structure, such as a stress critical component, in greater detail. The first approach to this end is to model the entire structure with a fine mesh. However, this is computationally expensive because a large number of equations must be solved. The second approach is grading a finer finite element mesh in certain areas than others, and this may require the use of transition zones using either triangular elements or specially formulated transition elements. The user may encounter problems generating this type of mesh, especially if a mesh generation preprocessor is being used. The third approach is to solve the problem by subregion modeling, such as the specified displacement method in ANSYS or the zooming method. As the stresses by these subregion modeling are also based on conventional displacement-based

finite element analysis, inter-element discontinuities in the stresses still remain.

In this study, with the application of the theory of conjugate approximations and Loubignac's iterative algorithm approximately to the local region, an efficient method to build an improved and continuous stress field without further refining the grid in local regions is proposed. To check the validity of the proposed method, stress analysis on two examples has been carried out.

2. DISPLACEMENT-BASED FINITE ELEMENT FORMULATION

In the conventional displacement-based finite element method, after a grid is generated over the entire domain, a continuous displacement distribution needs to be assumed for every element. For an element e, the shape function matrix of the element $[N]$ and the nodal displacement vector of the element $\{\Delta\}^e$ generally assume the displacement field: $\{u\}^e = [N]\{\Delta\}^e$.

The strain vector $\{\varepsilon\}^e$ and the stress vector $\{\sigma\}^e$ can be derived as $\{\varepsilon\}^e = [B]\{u\}^e$ and $\{\sigma\}^e = [D]\{\varepsilon\}^e = [D][B]\{u\}^e$, where $[B]$ is the element strain matrix and $[D]$ is the constitutive matrix of the material.

The system equation of an element is expressed as the virtual work principle $[K]^e\{\Delta\}^e = \{F\}^e$, where the stiffness matrix of the element is $[K]^e = \int_{\Omega_e} [B]^T [D][B]\, d\Omega_e$.

3. CONJUGATE APPROXIMATIONS

Brauchli and Oden [3] proposed the theory of conjugate approximations and applied the theory for continuous stress field representation in the conforming finite element model. To be brief, the conjugate stress idea is summarized as follows:

i) Conjugate stresses, $S^{ij\Delta}$, and the consistent nodal average, S^{ij}_{Δ}, are defined as follows:

$$S^{ij}_{\Delta} = \left\langle \sigma^{ij}, \Phi_{\Delta}(x) \right\rangle = \int_{\Omega} \sigma^{ij}\, \Phi_{\Delta}(x)\, d\Omega \tag{1}$$

$$S^{ij\Delta} = \left\langle \sigma^{ij}, \Phi^{\Delta}(x) \right\rangle = \int_{\Omega} \sigma^{ij}\, \Phi^{\Delta}(x)\, d\Omega \tag{2}$$

ii) The conjugated approximation functions $\Phi^{\Delta}(x)$ are expressed by the interpolation functions $\Phi_{\Delta}(x)$, which have the properties $\Phi_{\Delta}(x^{\Gamma}) = \delta^{\Gamma}_{\Delta}$: $\Phi^{\Delta}(x) = C^{\Delta\Gamma}\, \Phi_{\Gamma}(x)$.

Here $C^{\Delta\Gamma}$ is the inverse of the fundamental matrix $C_{\Delta\Gamma}$, defined as follows:

$$C_{\Delta\Gamma}\, S^{ij\Delta} = S^{ij}_{\Delta} \tag{3}$$

where $C_{\Delta\Gamma}$ is the fundamental matrix defined as the inner product of the shape functions over the whole domain: $C_{\Delta\Gamma} = \left\langle \Phi_{\Delta}(x), \Phi_{\Gamma}(x) \right\rangle = \int_{\Omega} \Phi_{\Gamma}(x)\, \Phi_{\Delta}(x)\, d\Phi$.

The major difficulty encountered in applying the theory of consistent stress approximations concerns the matrix $C_{\Delta\Gamma}$ of Eq. (3).

4. STRESS IMPROVEMENT IN THE LOCAL REGION

Figure 1 represents the whole domain, which consists of the local region, the outer region, and the interface. The finite element equation for the whole domain can be expressed

as follows, where the subscripts 1, 2, and 3 represent the local region, the interface, and the outer region, respectively.

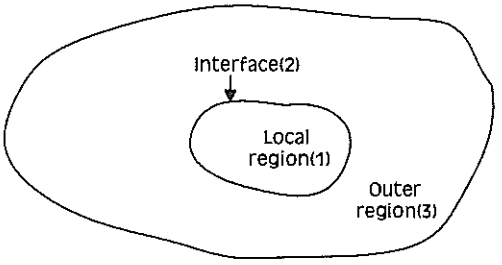

Fig.1 Illustration of the whole domain and the local region

$$\begin{bmatrix} K_{11} & K_{12} & 0 \\ K_{21} & K_{22} & K_{23} \\ 0 & K_{32} & K_{33} \end{bmatrix} \begin{Bmatrix} u_1 \\ u_2 \\ u_3 \end{Bmatrix} = \begin{Bmatrix} f_1 \\ f_2 \\ f_3 \end{Bmatrix} \tag{4}$$

Discarding the third equation in Eq. (4), the finite element equation involving only the local region and interface, expressed as subscript L, is as follows:

$$[K]_L \, u_L = f_L \tag{5}$$

where,

$$[K]_L = \begin{bmatrix} K_{11} & K_{12} \\ K_{21} & K_{22} \end{bmatrix}, \quad u_L = \begin{Bmatrix} u_1 \\ u_2 \end{Bmatrix}, \quad f_L = \begin{Bmatrix} f_1 \\ f_2 - K_{23}\, u_3 \end{Bmatrix}$$

Jara-Almonte and Knight [5] showed that by refining the mesh only in the local region and solving Eq. (5), an improved finite element solution could be obtained in the local region. However, in this study, an approximate method to improve the finite element solution in the local region has been proposed by combining the theory of conjugate approximations with Loubignac's iterative method and without further refining the grid in the local region [6]. Applying the conjugate approximation to the whole domain, as in Fig. 1, Eq. (3) can be expressed as follows:

$$\begin{bmatrix} C_{11} & C_{12} & 0 \\ C_{21} & C_{22} & C_{23} \\ 0 & C_{32} & C_{33} \end{bmatrix} \begin{Bmatrix} S^1 \\ S^2 \\ S^3 \end{Bmatrix} = \begin{Bmatrix} S_1 \\ S_2 \\ S_3 \end{Bmatrix} \tag{6}$$

where S^i represents the conjugate stress, $S^{ij\Delta}$, defined in Eq. (2) and S_i represents the consistent nodal S^{ij}_{Δ} defined in Eq. (1). Discarding the third equation in Eq. (6), and supposing that the conventional nodal stress averages (σ_3) in the outer region can replace the conjugate stresses (S^3), Eq. (6) can be approximately reduced as follows:

$$\begin{bmatrix} C_{11} & C_{12} \\ C_{21} & C_{22} \end{bmatrix} \begin{Bmatrix} S^1 \\ S^2 \end{Bmatrix} = \begin{Bmatrix} S_1 \\ S_2 - C_{23}\, S^3 \end{Bmatrix} \approx \begin{Bmatrix} S_1 \\ S_2 - C_{23}\, \sigma_3 \end{Bmatrix} \tag{7}$$

Using Eq. (5) and Eq. (6), an improved stress field that is continuous can be obtained by following iterative procedure:

i) Solve Eq. (5) to obtain u_L

ii) Calculate the conventional stress $\sigma_L = [D][B]u_L$

iii) Solve Eq. (7) to obtain the conjugate stress S^i

iv) Interpolate the continuous stress field using S^i and the shape function N^*: $\sigma^* = N_i^* S^i$.

v) Compute the nodal force vector that corresponds to the continuous stress field, σ^* :

$$f_e = \int_{\Omega_e} [B]^T \sigma^* \, d\Omega_e = \int_{\Omega_e} [B]^T N^* \, d\Omega_e \, S^i \ , \ f^* = \sum_{element} f_e = \sum_{element} \int_{\Omega_e} [B]^T \sigma^* \, d\Omega_e = \sum_{element} \int_{\Omega_e} [B]^T N^* \, d\Omega_e \, S^i$$

The L_2-norm of force-imbalance, $\|\Delta f\|_i$ and the ratio of the L_2-norm of force-imbalance, R_i, at the *i-th* iteration are defined as follows:

$$\|\Delta f\|_i^2 = \int_\Omega \left(f - f^*\right)^T \left(f - f^*\right) d\Omega \ , \ R_i = \frac{\|\Delta f\|_i}{\|\Delta f\|_0}$$

vi) Solve $\Delta u_L^i = K^{-1}\left(f_L - f^*\right)$

vii) Update u_L and σ_L

$$u_L^{i+1} = u_L^i + \Delta u_L^i \ , \ \sigma_L^{i+1} = [D][B]u_L^{i+1}$$

viii) Go to step iii) unless $\|\Delta u_L^i\|$ is less than a predefined value.

The total strain energy (U_{Total}) expression from the continuous stress field is obtained as $U_{Total} = \|u\|_i \equiv \frac{1}{2}\int_\Omega \sigma^{*T} \varepsilon^* \, d\Omega = \frac{1}{2}\int_\Omega \sigma^{*T} D^{-1} \sigma^* \, d\Omega$

5. DETERMINATION OF THE LOCATION AND SIZE OF THE LOCAL REGION

For a given element *i*, the *local strain energy density* ($LSED_i$) is defined as $LSED_i = \frac{U_i}{A_i}$.

where U_i and A_i are the strain energy and the area(or volume) in an element *i*, which are from the conventional finite element solution, respectively.

Similarly, for the whole domain, the *global strain energy density* ($GSED$) is defined as: $GSED = \frac{Total\ strain\ energy\ of\ the\ system}{Total\ volume(or\ area)\ of\ the\ system}$

Many researchers [7,8,9] have proposed the strain energy density as an indicator for looking for the location of high-stress concentrations or singularities. In this study, the *strain energy density index* ($SEDI$: β_i) for each element is used to discern the location and the size of the local region model, $\beta_i = \frac{LSED_i}{GSED}$.

6. NUMERICAL EXAMPLES

6.1 Thick-walled Cylinder

To show that the present method is effective for smooth problems, a thick-walled cylinder problem subjected to uniform internal pressure under plane strain conditions is considered. Due to symmetry, one quarter of the cylinder is taken for analysis, as shown in Fig. 2. Poisson's ratio (ν) and Young's modulus (E) are taken to be 0.3 and 1.0Pa, respectively. The finite element model of the problem with quadrilateral plane strain element is shown in Fig. 2 and the shaded region in Fig. 2 represents the local region model (submodel) discerned by $SEDI$ whose value is above 1.0. The exact solution [10] is compared with various stress solutions, which come from ANSYS [11] and the present method, over the whole domain and the local region model.

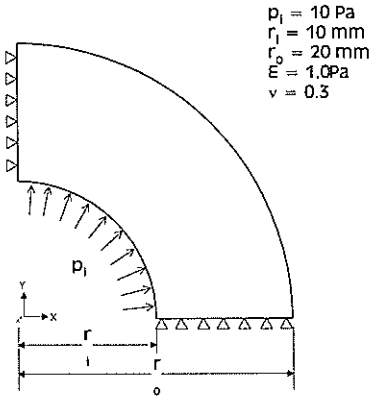

Fig. 2(a) Thick-walled cylinder under internal pressure

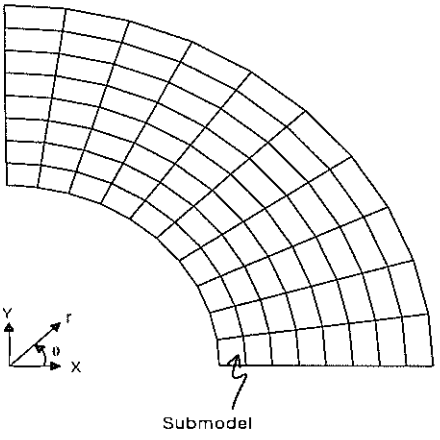

Fig. 2(b) Finite element model

To show that the present method is effective for smooth problems, a thick-walled cylinder problem subjected to uniform internal pressure under plane strain conditions is considered. Due to symmetry, one quarter of the cylinder is taken for analysis, as shown in Fig. 2. Poisson's ratio (ν) and Young's modulus (E) are taken to be 0.3 and 1.0Pa, respectively. The finite element model of the problem with quadrilateral plane strain element is shown in Fig. 2 and the shaded region in Fig. 2 represents the local region model (submodel) discerned by *SEDI* whose value is above 1.0. The exact solution [10] is compared with various stress solutions, which come from ANSYS [11] and the present method, over the whole domain and the local region model.

Figure 3 shows the variation of the "ratio of L_2-norm of force imbalance", R_l, as iteration numbers in the whole domain and the local region model. Figure 3 shows that R_l are monotonously decreasing and rapidly converging in a few iterations. This means that the iterative procedure could effectively improve the stress and displacement field, both for the whole domain and the local region model to meet the finite element equilibrium equation. Figure 4 shows the comparison of the radial stresses (σ_r) along the inner radius, which are computed with iteration in the local region and the whole domain model from the present study with the exact solution and the conventional finite element solution (ANSYS results). Four observations are inferred from Fig. 4. First, the nodal stress averages from ANSYS are 21.53% lower than the exact solution for the finite element model of Fig. 2(b), whose maximum node number is 99 and element length is h. In the refined finite element model whose maximum node number is 357 and element length is $\frac{1}{2}h$, the nodal stress averages from ANSYS are 11.31% lower than the exact solution. The stress results from the present study, whether they are from the whole domain model or local region model, are at most 3.47% lower than the exact solution. This shows that the present study can improve the accuracy of the stress figures greatly. Second, the radial stresses (σ_r) from the pure conjugate approximations, i.e., without iteration, are not only 13.6% lower than the exact solution but also 2.3% lower than the nodal stress averages from the refined finite element model. Third, the stress from the local region model is in agreement with that of the whole domain model, except for the presence of a few more oscillations, even though oscillations are also observed in the whole domain model. It seems that the additional oscillations in the local region model are attributed to the assumption that the displacement

field (u_3) and stress field (σ_3) in the outer region is fixed, while in fact they may vary at each iteration. Fourth, the total strain energy is monotonously increasing and rapidly converging into the exact solution [10] as the number of iteration increase.

In addition, the computing time of the local region model is significantly reduced, compared with that of the whole domain model. Based on the Cyber-960, the computing time for the local region model, whose maximum node number is 33, is 7.076 *sec.*, while that for the whole domain model, whose maximum node number is 99, is 316.052 *sec.* until R_i reaches below 0.1.

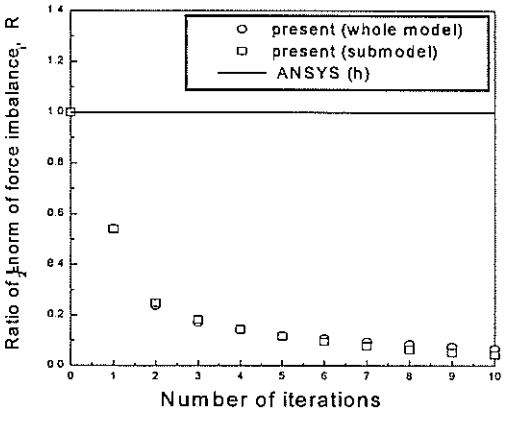

Fig. 3 Ratio of L_2-norm of force imbalance vs. number of iterations

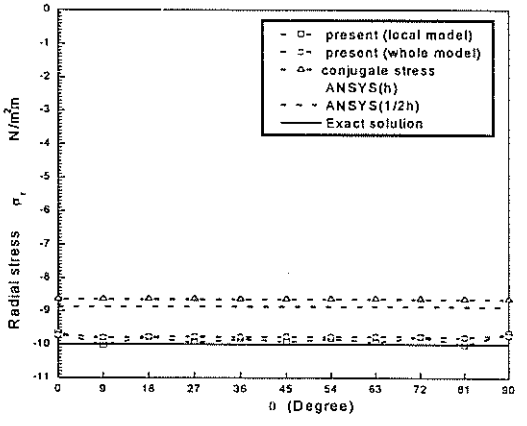

Fig. 4 Variation of the radial stress along the inner radius

6.2 Infinite Plate with a Central Circular Hole Subjected to Uniaxial Tensile Loads

In the second example, an infinite plate with a central circular hole subjected to a far-field tensile load, $\sigma = 1.0\,\mathrm{N/mm^2}$, is considered. Due to symmetry, one-quarter of the cylinder is taken for analysis, as shown in Fig. 5(a). Poisson's ratio and Young's modulus are taken to be 0.3 and 1000Pa, respectively. Plane stress conditions are assumed and boundary conditions are described so that the symmetry conditions are satisfied. The stress boundary conditions [10] are specified along each boundary as follow:

Along BC and CD

$$\sigma_x = 1 - \frac{a^2}{r^2}\left(\frac{3}{2}\cos 2\theta + \cos 4\theta\right) + \frac{3}{2}\frac{a^4}{r^4}\cos 4\theta$$

$$\sigma_y = -\frac{a^2}{r^2}\left(\frac{1}{2}\cos 2\theta - \cos 4\theta\right) - \frac{3}{2}\frac{a^4}{r^4}\cos 4\theta$$

$$\tau_{xy} = -\frac{a^2}{r^2}\left(\frac{1}{2}\sin 2\theta + \sin 4\theta\right) + \frac{3}{2}\frac{a^4}{r^4}\sin 4\theta$$

$a = 1.0$

Along AB and ED

$$\tau_{xy} = 0$$

Along AE

$$\sigma_r = \tau_{r\theta} = 0$$

Figure 5(b) represents the finite element model with quadrilateral plane stress elements, where the shaded region represents the local region model. Figure 6 represents the variation of R_i as iteration numbers for the whole domain model whose maximum number is 325

and for the local region model whose maximum number is 125.

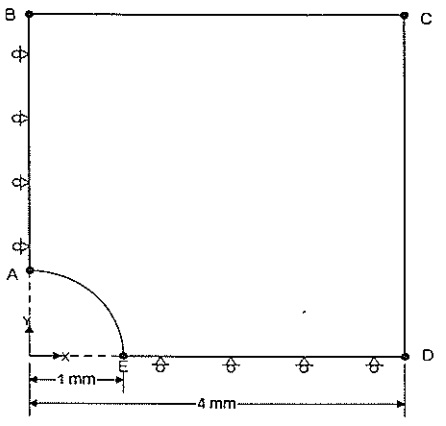

Fig. 5(a) Infinite plate with a hole subjected to uniaxial tensile loads

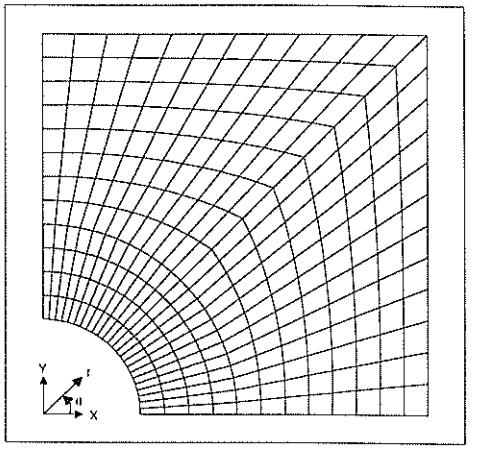

Fig. 5(b) Finite element model

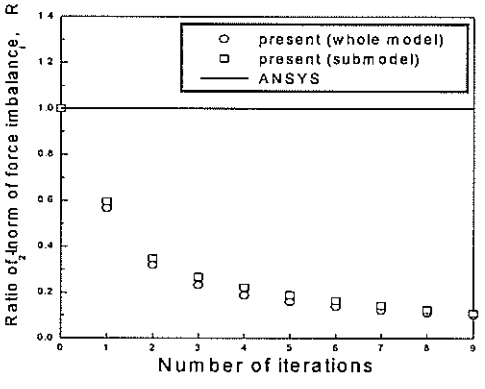

Fig. 6 Ratio of L_2-norm of force imbalance vs. number of iterations

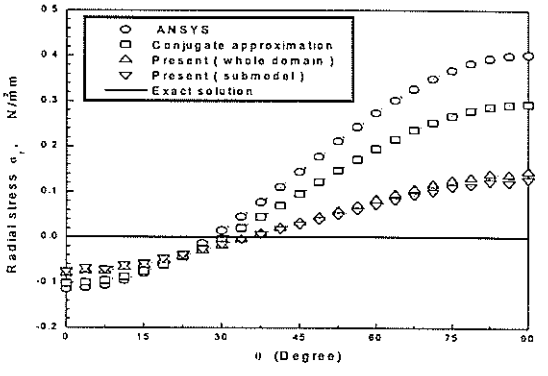

Fig. 7 Variation of the radial stress along the inner radius

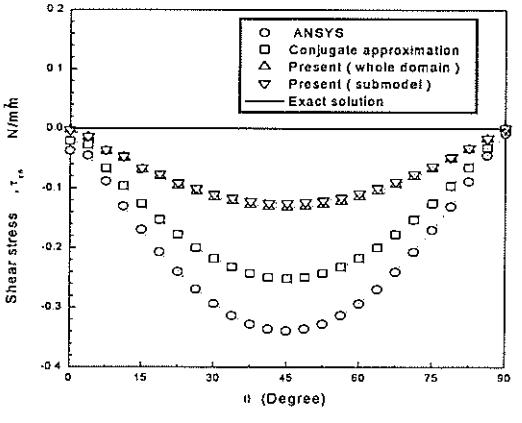

Fig. 8 Variation of the shear stress along the boundary AE domain

Figure 6 shows that R_i significantly decreases and converges in a few iterations. This denotes that the stress fields are being improved to satisfy the finite element equilibrium equation at the little additional cost of computing time. Figures 7 and 8 represent the variation of σ_r and $\tau_{r\theta}$ along the boundary AE, respectively. Two observations are inferred from Figs. 7 and 8. First, the conjugate stresses are more accurate in approximating the exact solution than the conventional finite element solution. Second, the lack of significant stress differences in the local region model and whole domain model implies that the present study is effective in building an improved and continuous stress field in the local region.

7. CONCLUSIONS

Based on the displacement-based finite element solution, an approximate method to build an improved and continuous stress field in the local region has been proposed without further refining the grid. Numerical test through two examples shows that the stress fields from the whole domain model and the local region model were both improved to satisfy the finite element equilibrium equation and converged in a few iterations. In addition, the results show that the stress field from the local region model is seldom different from that of the whole domain model. And computing time to obtain the stress field for the local region model is considerably reduced compared with that for the whole domain model. Therefore the present method can be used to predict an improved and continuous stress field, both effectively and economically, in the local region where detailed stress analysis is required.

ACKNOWLEDGEMENTS

This Project has been carried out under the Nuclear R&D Program by MOST.

REFERENCES

1. Taylor, R. L. and Zienkiewicz, O. C., Mixed finite element solution of flow problems, Chapter 1, *Finite Elements in Fluids*, Vol. 4 (ed. Gallagher, R. H. *et al.*), Wiley, Chichester, 1982..
2. Hinton, E. and Campbell, J. S., *Int. J. Numer. Meth. Engng.*, Vol. 8, pp. 461- 480, 1974.
3. Brauchli, H. J. and Oden, J. T., *Quarterly of Applied Mathematics*, No. 1, pp. 65–90, 1971.
4. Loubignac, G., Cantin, G., and Touzot, G., *AIAA Journal*, Vol. 15, pp. 1645 –1646, 1977.
5. Jara-Almonte, C. C. and Knight, C. E., *Int. J. Numer. Meth. Engng.*, Vol. 26, pp. 1567-1578, 1988.
6. Song, K. N., *KSME International Journal*, Vol. 12, pp. 859-870, 1998.
7. Febres-Cedillo, H. E. and Asghar Bhatti, M., *Comput. Struct.*, Vol. 28, pp. 523-533, 1988 .
8. Botkin, M. E. and Bennet, J. A, The application of adaptive mesh refinement to shape optimization of plate structures, in *Accuracy Estimates and Adaptive Refinements in Finite Element Computations*, (ed. Babuska, I., Zienkiewicz, O. C., Gago, J., and de A. Oliviera, E. R.), John Wiley & Sons, Chichester, pp. 227-246, 1986.
9. Lee, C. K. and Lo, S. H., *Int. J. Numer. Meth. Engng.*, Vol. 35, pp. 1967-1989, 1992.
10. Timoshenko, S. P., *Theory of Elasticity*, 3rd ed., McGraw-Hill Kogakusha, Tokyo, pp. 68- 90,1970.
11. *ANSYS User's Manual for Revision 5.0*, Swanson Analysis System, Inc., 1992.